Neuropsychopharmacology (2013) 38, 1438–1450

www.neuropsychopharmacology.org

$GABA_A$ Receptors Predict Aversion-Related Brain Responses: An fMRI-PET Investigation in Healthy Humans

Dave J Hayes*[,1], Niall W Duncan[1,2], Christine Wiebking[1,3], Karin Pietruska[4], Pengmin Qin[1], Stefan Lang[1], Jean Gagnon[5], Paul Gravel BIng[6], Jeroen Verhaeghe[6], Alexey P Kostikov[6], Ralf Schirrmacher[6], Andrew J Reader[6], Julien Doyon[7], Pierre Rainville[4,7] and Georg Northoff[1]

[1]Mind, Brain Imaging and Neuroethics, Institute of Mental Health Research, Royal Ottawa Health Care Group, University of Ottawa, Ottawa, ON, Canada; [2]Department of Biology, University of Carleton, Ottawa, ON, Canada; [3]Department of Biology, Freie Universität, Berlin, Germany; [4]Faculté de médecine dentaire, Université de Montréal, Pavillon Paul G. Desmarais, Montréal, QC, Canada; [5]Centre de réadaptation Lucie-Bruneau, Université de Montréal, Montréal, QC, Canada; [6]McConnell Brain Imaging Centre, Montreal Neurological Institute, McGill University Montreal, Montréal, QC, Canada; [7]Functional Neuroimaging Unit, Department of Psychology, Université de Montréal, Montréal, QC, Canada

The perception of aversive stimuli is essential for human survival and depends largely on environmental context. Although aversive brain processing has been shown to involve the sensorimotor cortex, the neural and biochemical mechanisms underlying the interaction between two independent aversive cues are unclear. Based on previous work indicating ventromedial prefrontal cortex (vmPFC) involvement in the mediation of context-dependent emotional effects, we hypothesized a central role for the vmPFC in modulating sensorimotor cortex activity using a GABAergic mechanism during an aversive–aversive stimulus interaction. This approach revealed differential activations within the aversion-related network (eg, sensorimotor cortex, midcingulate, and insula) for the aversive–aversive, when compared with the aversive–neutral, interaction. Individual differences in sensorimotor cortex signal changes during the aversive–aversive interaction were predicted by $GABA_A$ receptors in both vmPFC and sensorimotor cortex. Together, these results demonstrate the central role of GABA in mediating context-dependent effects in aversion-related processing.
Neuropsychopharmacology (2013) **38,** 1438–1450; doi:10.1038/npp.2013.40; published online 13 March 2013

Keywords: fMRI; PET; flumazenil; human; perigenual anterior cingulate cortex; emotion

INTRODUCTION

Understanding aversive processing in the brain is necessary for fully grasping the underlying principles of emotional brain function. Brain-imaging studies using the passive presentation of unpleasant stimuli have identified regions, such as the motor and anterior cingulate cortices, insula, striatum, amygdala, and periaqueductal gray, as being consistently responsive to aversive stimuli of various sensory modalities (Grupe *et al*, 2012; Nitschke *et al*, 2006). Importantly, findings from these studies are highly consistent with those found in animal studies (see Hayes and Northoff, 2011 for review). However, aversion-related imaging studies have focused almost entirely on mapping the elicited aversive responses from the brain, whereas the impact of context on the basal processing of aversive stimuli remains unclear. The mapping of such an interaction at the level of the whole brain will likely contribute to a fundamental understanding of how the underlying neural context shapes our perception of aversive stimuli. For instance, the same aversive stimulus may be processed differently in the presence of other aversive or rewarding stimuli. However, the neural underpinnings of such interactions remain unclear.

Although not fundamental for basal valuative processing, the human ventromedial prefrontal cortex (vmPFC) was recently hypothesized to be essential in integrating emotion-related contextual information (Roy *et al*, 2012). Most research investigating the context dependence of aversion has focused on fear learning in rodents (Ciocchi *et al*, 2010; Johnson *et al*, 2011). These paradigms typically involve the pairing of initially neutral environmental cues to the exposure of an aversive stimulus (eg, electric shock)—whereby the cues alone eventually result in aversive responses. These studies have contributed greatly to an understanding of aversive learning mechanisms at the microcircuit level and, indeed, congruent findings have been noted at the macroscopic level in humans (Delgado *et al*, 2011). The role of the prefrontal cortex in response to threatening stimuli has also been noted in rodents (Chan *et al*, 2011; Thompson *et al*, 2010), and there is evidence that context-dependent aversion-related activity may involve GABAergic function (Fiorelli *et al*, 2008; Lehner *et al*, 2010).

*Correspondence: Dr DJ Hayes, Mind, Brain Imaging and Neuroethics, Institute of Mental Health Research, Royal Ottawa Health Care Group, University of Ottawa, 1145 Carling Avenue, Room 6441, Ottawa, ON K1Z 7K4, Canada, Tel: +613 722 6521; extension 6625, Fax: +613 798 2982, E-mail: david.hayes@theroyal.ca
Received 2 January 2013; revised 21 January 2013; accepted 29 January 2013; accepted article preview online 6 February 2013

While there is an abundance of animal research regarding the role of GABA in aversive processing (Hayes *et al*, 2011; Lehner *et al*, 2008), few studies in healthy humans have made this link, although one study showed elevations in human vmPFC GABA levels following a painful stimulus (Kupers *et al*, 2009). This is in spite of the knowledge that the anxiolytic effects of socially consumed alcohol and clinically prescribed benzodiazepines are linked to their positive modulatory effects on the inhibitory ionotropic GABA$_A$ receptor (GABA$_A$R). Furthermore, novel drugs targeting the GABA$_A$R have been developed and proposed for use against pain, depression, and other neuropsychiatric disorders associated with alterations in aversive processing (Rudolph and Knoflach 2011). Despite this knowledge, surprisingly little is known about the role of GABA$_A$Rs in context-dependent aversive processing in healthy people.

As studies in humans have only begun to consider aversive processing at the whole-brain level (Hayes and Northoff 2012; Hayes and Northoff 2011; Nitschke *et al*, 2006), and none to date have investigated the modulatory impact of preestablished conditioned stimuli on this network activity, the first aim of our study used a novel approach in humans to better understand this aversive context interaction. This was done by determining whether aversion-related network activity elicited by the anticipation of an ankle shock could be modulated by a learned cue (ie, passive exposure to an aversive or neutral preconditioned tone), which, importantly, had no bearing on the probability of receiving a shock. Moreover, given the evidence in animals of GABAergic involvement in context-dependent aversive processing, as well as the potential role of the vmPFC, our second aim was to investigate the relationship between intra-regional and vmPFC GABA$_A$R binding potentials (BPs; using ^{18}F-radiolabelled flumazenil (FMZ) in positron emission tomography (PET)) and the context-dependent aversion-related blood oxygenation level-dependent (BOLD) responses noted in Aim 1.

In summary, the present study had two main aims. The first aim identified brain regions involved in an aversive context interaction: how aversion-related network activity, induced by the threat of certain shock or certain 'safety', could be modulated using a cue (ie, the presentation of aversive or neutral tones conditioned before the scanning session). The second aim investigated the relationship between intra-regional and vmPFC GABA$_A$Rs and fMRI context-related BOLD responses identified in the first aim. Taken together, this multimodal approach aimed to better characterize the brain-based and biochemical underpinnings of context-dependent aversive processing in humans.

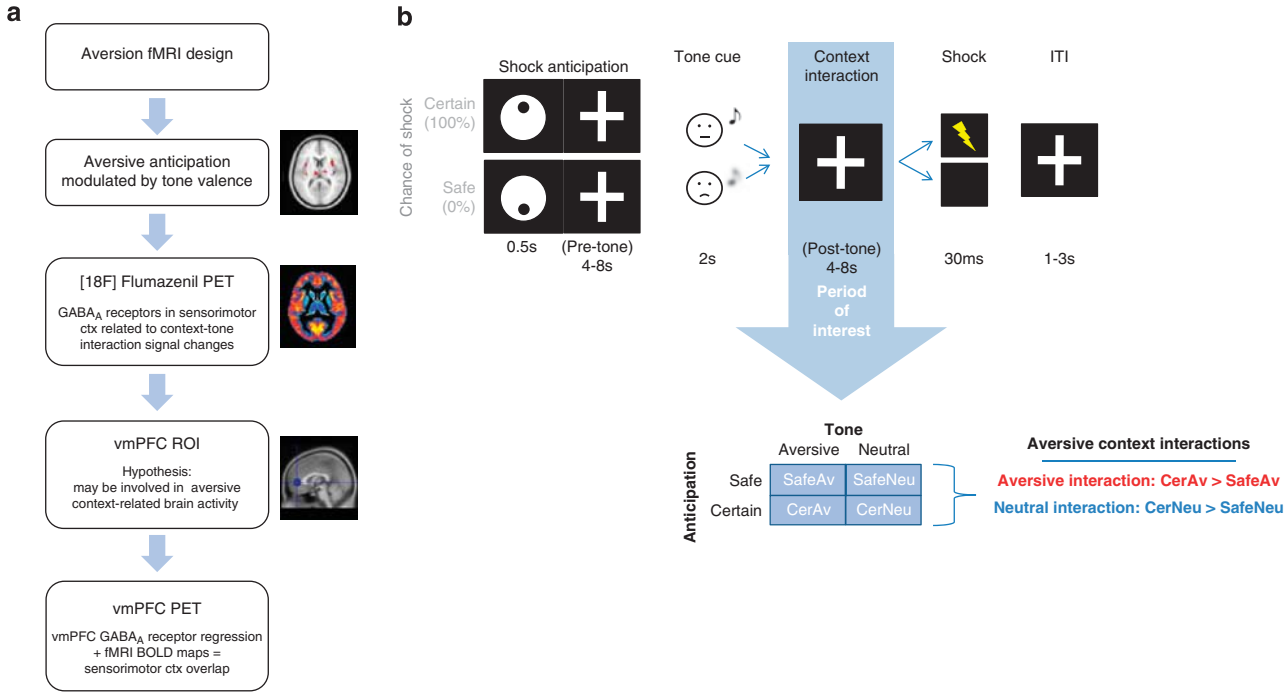

Figure 1 Aversion context interaction study. (a) Study overview: the main steps and methodologies used in the present study are outlined. (b) fMRI design: outline of stimuli order experienced by subject in scanner (above), Shock context indicator is followed immediately by fixation cross (which lasts the duration of the trial)which marks the pretone period, and which is followed by a conditioned tone (illustrated here as: neutral tone = neutral face with note; aversive tone = sad face with fuzzy note) period. Next is the aversive context interaction period of interest (indicated by blue arrow) from which two interaction contrasts were analyzed: aversive interaction (CerAv > SafeAv) and neutral interaction (CerNeu > SafeNeu). The trial ends with a shock or no shock followed by a brief intertrial interval (ITI; 1-3s). Only two visual stimuli, the context indicator and the fixation cross, are ever experienced by the subject. Stimuli are not drawn to scale. CerAv, fixation period of interest during shock anticipation following the presentation of the aversive tone; CerNeu, fixation period of interest during shock anticipation following the presentation of the neutral tone; ctx, cortex; fMRI, functional magnetic resonance spectroscopy; GABA$_A$, gamma-aminobutyric acid A receptors; PET, positron emission tomography; SafeAv, fixation period of interest during no shock anticipation following the presentation of the aversive tone; CerNeu, fixation period of interest during no shock anticipation following the presentation of the neutral tone; vmPFC, ventromedial prefrontal cortex.

MATERIALS AND METHODS

Participants

A total of 28 healthy participants (10 female, mean age 22 ± 4 years; range 18–32), recruited from McGill University and the Université de Montréal, underwent fMRI and PET (Figure 1a). All potential participants were screened for a history of psychiatric, neurological, or other medical disorders using a semi-structured clinical questionnaire. All participants gave their written informed consent and were monetarily compensated for their participation. Ethics approval was granted from the local ethics committees at each respective university.

From the initial group of 28, 4 were removed from further fMRI analysis because of technical challenges/anatomical artefacts or excessive head movement (>2 mm), leaving 24 participants (8 female; age 22 ± 4 years); 4 additional subjects were removed from PET analysis for similar reasons, leaving 20 participants for combined PET-fMRI analysis (7 female; age 23 ± 4 years). Additional information related to all Materials and methods can be found in the Supplementary Material.

Tone Conditioning

Participants were passively conditioned to two distinct tones (65 dB sine waves of 700 and 1300 Hz; 5–8 s duration; 1–4 s intertrial interval) in a mock scanner via fMRI compatible headphones (model S14; Sensimetrics, Malden, MA) using parameters adapted from Dunsmoor *et al*, 2008 and Knight *et al*, 2009. The conditioned stimuli (aversive tone co-terminating randomly 50% of the time with a 100 dB white noise burst, 500 ms, with rise time <1 ms; neutral tone never followed by white noise burst) were counterbalanced and pseudorandomly presented 168 times each over a 50-min period. The aversive and neutral conditioned tones were rated by each subject for their unpleasantness (on a scale of 0–100) following each of four runs.

Electrical Stimulation and Electrodermal Activity Measures Acquisition and Analysis

Parameters and instruments for transcutaneous electrical stimulation were similar to those used by Piche *et al*, (2010). Electrodermal activity (EDA) was recorded using Acqknowledge software (version 4.1; Biopac Research Systems, CA) using Ag-AgCl electrodes placed on the bottom of the left foot. The onset and tracking of the fMRI paradigm was signaled by TTL pulses and recorded simultaneously in a separate Acqknowledge channel for later analysis. EDA was analyzed with SCRalyze 2.1.2b (scralyze.sourceforge.net), which employs a general linear model for event-related evoked skin conductance responses (Bach *et al*, 2010; Bach *et al*, 2009). The EDA, originally sampled at 1000 Hz, was band pass filtered (using a first-order Butterworth filter and cutoff frequencies of 0.0159 and 5 Hz), down sampled to 10 Hz, and *z*-transformed to account for between-subjects amplitude variance. Results are parameter estimates (in arbitrary units) of the mean response amplitude for each experimental condition (Bach *et al*, 2010). The data were analyzed statistically using SPSS 17 (SPSS, Chicago, IL) with a 2 (context: safe, certain) $\times$ 2 (tone: neutral, aversive) repeated measures ANOVA.

Aversion Context Interaction fMRI Paradigm

As outlined in Figure 1b, the start of each trial was indicated by an icon denoting the probability of receiving electrical stimulation at the end of the trial (safe: 0%, certain: 100%). This was followed immediately by a fixation cross that remained until the end of the trial (total trial time = 12–22 s). The period of interest (Figure 1b; blue arrow) was chosen to investigate whether the aversion-related activity produced through the anticipation to an upcoming aversive stimulus, using a safe or certain shock indicator, can be modulated by a cue (ie, the presentation of a neutral or aversive conditioned tone) that does not have an impact on the probabilistic outcome of shock itself. This context interaction period focused on the modulatory impact of the conditioned tone on the activations related to the shock anticipation.

This interaction approach resulted in four independent events as follows: no shock anticipation following an aversive (SafeAv) or neutral (SafeNeu) tone or certain shock anticipation following an aversive (CerAv) or neutral (CerNeu) tone. There were 25 repetitions per condition across four runs for a total time of 51 min. For improved design orthogonality, trials in which the tone was omitted from the safe or certain conditions (25 times for each) and 4 trials in which the white noise burst followed the aversive tome (as in the prescanning conditioning phase) were included. Jittered intertrial intervals (1–3 s; 125 across all four runs) were also included. As noted above, the paradigm was explained to the subjects in detail such that they were clearly aware of the non-contingent nature of the tone cue on the outcome of shock (ie, the tone type was presented randomly and did not provide any information about the impending shock or subsequent trials).

fMRI Data Analysis

The effect of the aversive and neutral cues on shock-related anticipation was examined using the following context interaction contrasts: Av(Cer > Safe) for the aversive interaction and Neu(Cer > Safe) for the neutral interaction. To further identify regions that were spatially selective for the aversive interaction, the contrast was masked ($\neg$) with the neutral interaction contrast at the same threshold using the expression (Av(Cer > Safe))$\neg$(Neu(Cer > Safe)). The regions selective for the neutral interaction using the expression (Neu(Cer > Safe)) $\neg$ (Av(Cer > Safe)), and those regions that overlapped/intersected using the expression (Av(Cer > Safe)) $\cap$ (Neu(Cer > Safe)), were also determined.

Regions in this analysis were considered significant at the conservative level of $p<0.05$, FWE-corrected, $k \geqslant 10$. The anatomical localization of significant activations in the main resulting aversive interaction contrast (CerAv > SafeAv) and neutral interaction contrast (CerNeu > SafeNeu) were assessed by superimposition of the SPM maps on a standard template. Regions were identified and labeled macroanatomically by the FSL probabilistic Harvard-Oxford atlas (FMRIB's Software Library, http://www.fmrib.ox.ac.uk/fsl/) (Smith *et al*, 2004). Percent signal changes

from the resulting clusters were extracted using the MarsBaR toolbox (http://www.sourceforge.net/projects/marsbar).

PET Acquisition and Reconstruction

In all, 20 subjects (from the total of 28 as mentioned above) underwent PET imaging with FMZ, a competitive antagonist at the benzodiazepine-binding site on the $GABA_AR$. It is a common *in vivo* method used to measure $GABA_AR$ BP (a combined measure of density of available receptors and their affinity; it reflects the ratio at equilibrium of specifically bound to non-displaceable radioligand using the pons white matter as a reference region) in humans (Frey *et al*, 1991; Salmi *et al*, 2008). Image analysis was similar to that described elsewhere (Wiebking *et al*, 2012).

Combined Analysis

In a first step, regions of interest (ROIs) from the aversive (Av(Cer > Safe))¬(Neu(Cer > Safe)) and neutral (Neu(Cer > Safe))¬(Av(Cer > Safe)) interaction regions were identified (Figure 2a; Table 1; Supplementary Table S1), and percent signal change differences in each of the functional conditions (ie, CerAv > SafeAv and CerNeu > SafeAv following the termination of the tone; Cer > Safe before the tone onset) were extracted (Figure 2b for an illustration of selected regions; Supplementary Table S2 for all values). $GABA_AR$ BPs from these regions were extracted using FSL

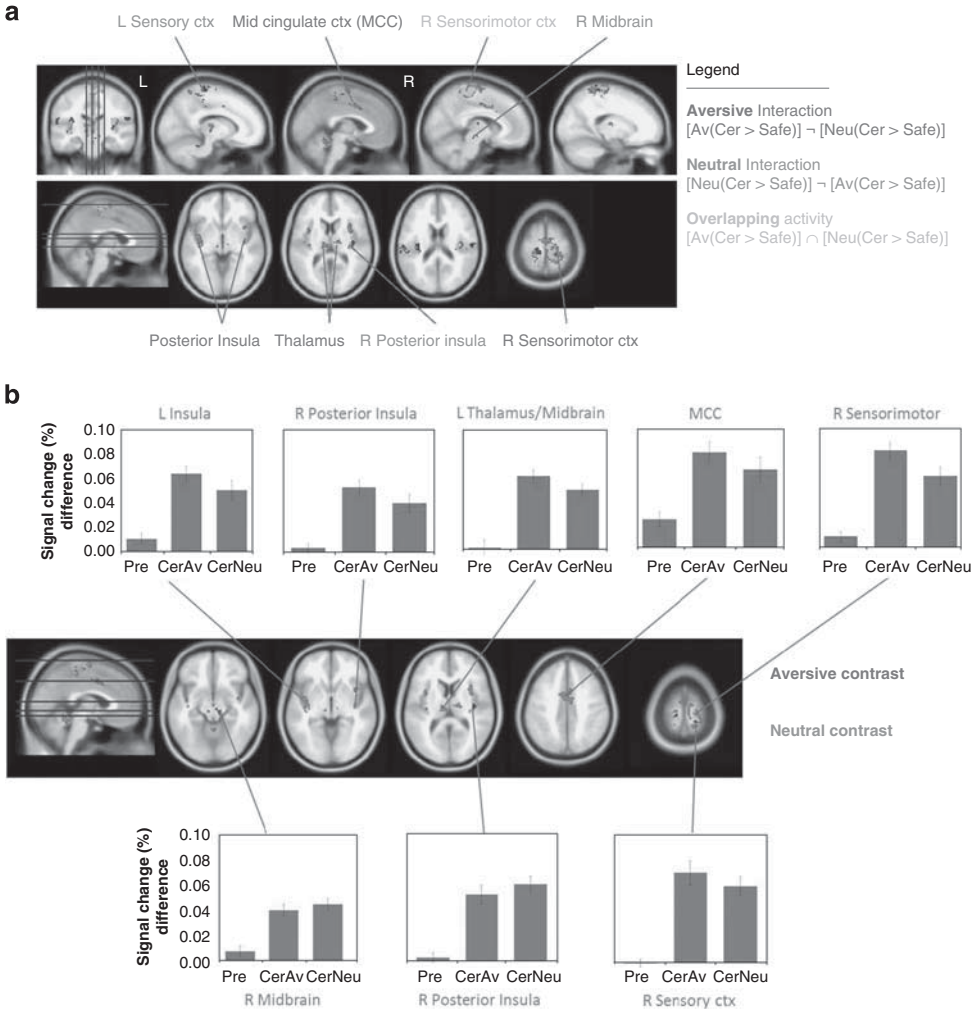

Figure 2 Aversion context BOLD activity interactions. (a) BOLD activity for context interactions: regions showing activations specific to the aversive interaction contrast [Av(Cer > Safe)] ¬ [Neu(Cer > Safe)] (ie, the positive interaction between shock anticipation and the aversive tone) are shown in red. Regions specific to the neutral interaction contrast [Neu(Cer > Safe)] ¬ [Av(Cer > Safe)](ie, the positive interaction between shock anticipation and the neutral tone) are shown in blue. Overlapping regions activated by shock anticipation following both aversive and neutral tones [Av(Cer > Safe)] ∩ [Neu(Cer > Safe)] are shown in green. All maps are voxel-wise FWE whole-brain corrected at $p < 0.05$, $k > 10$. ¬ represents the masking/negation/subtraction of a contrast with another; ∩ represents the overlap or intersection of clusters. See Table 1 for coordinates and Supplementary Table S1 for supporting information. (b) selected mean signal changes (%) for context interaction regions. signal changes from aversion interaction (red) and neutral interaction (blue) regions for the two functional target contrasts (ie, CerAv: CerAv > SafeAv, CerNeu: CerNeu > SafeNeu), as well as for the pretone contrast (Pre: Pre Cer > Safe), are shown. Error bars represent standard error of the mean. See Table S2 for supporting information. Av, aversive conditioned tone; Cer, certain shock; ctx, cortex; MCC, mid cingulate cortex; Neu, neutral conditioned tone; R/L, left/right; Safe, certain absence of shock. See the web version for full colour images.

Table 1 Interaction Between Aversive Anticipation and Conditioned Tones

Certain > < Safe (voxel-wise FWE-corrected at $p < 0.05$)

Aversive interaction (Av(Cer > Safe))¬(Neu(Cer > Safe))				Neutral interaction regions (Neu(Cer > Safe))¬(Av(Cer > Safe))				Overlapping regions (Av(Cer > Safe))∩(Neu(Cer > Safe))			
Region	**Coordinates (x/y/z)**	**Volume (mm)**	**Cluster size**	**Region**	**Coordinates (x/y/z)**	**Volume (mm)**	**Cluster size**	**Region**	**Coordinates (x/y/z)**	**Volume (mm)**	**Cluster size**
L sens	−13, −46, 63	792	99	L sensorimotor/L PCC	−10, −31, 63	1224	153	L sens	−17, −34, 70	136	17
L sensorimotor	−18, −31, 69	544	68	L motor	−17, −40 69	152	19				
R sensorimotor	11, −28, 67	6576	822	R sens	16, −37, 76	184	23	R sensorimotor	9, −30, 66	6504	813
				R sens	18, −34, 67	168	21				
L post ins	−38, −7, 0	2264	283	L post ins	−34, −23, 18	520	65	L post ins	−38, −18, −5	296	37
				L post ins	−39, −22, −2	112	14				
R post ins	37, −10, −7	328	41	R post ins	39, −17, 11	640	80	R post ins	35, −19, 15	864	108
R anterior/mid ins	36, 8, 7	920	115								
R mid ins	38, 11, −4	128	16								
L central operculum	−55, 2, 3	432	54	L par oper	−53, −30, 20	1184	148	L par oper	−49, −35, 25	104	13
L sensassoc/par oper/SMG	−58, −25, 21	504	63								
R sensassoc/par oper/SMG	56, −28, 27	808	101								
R par oper/post Ins	34, −23, 18	272	34	R central oper	59, −17, 19	552	69	R par oper	49, −25, 20	184	23
R midbrain	9, −19, −8	208	26	R midbrain	9, −22, −12	120	15				
Cerebellum(culmen)	0, −49, −16	776	97	L cerebellum (culmen)	−9, −42, −25	200	25	Cerebellum (culmen)	1, −46, −20	104	13
MCC	2, 2, 41	2672	334								
L SMG/Inf parietal	−53, −34, 32	312	39								
L thal/midbrain	−9, −20, 3	1000	125								
R thal	14, −14, 11	360	45								
L PCC	−14, −28, 39	88	11								
		Total voxels	2373			Total voxels	632			Total voxels	1024

Regional information related to the aversive interaction contrast [Av(Cer > Safe)] ¬ [Neu(Cer > Safe)], the neutral interaction contrast [Neu(Cer > Safe)] ¬ [Av(Cer > Safe)], and the overlapping regions activated by shock anticipation followed by conditioned tones [Av(Cer > Safe)] ∩ [Neu(Cer > Safe)]. See Figure 2a for related BOLD maps.

such that intra-regional Pearson's correlations between BPs and signal changes across each interaction contrast could be performed (Table 2).

In a second step, a spherical ROI was created for the vmPFC (Figure 3a; $x = 0$, $y = 46$, $z = 2$; radius = 10 mm; total volume = 4120 mm^3), corresponding to previous reports (Duncan *et al*, 2011; Qin and Northoff, 2011). The GABA$_A$R BP from this region was also extracted from each subject. For whole-brain analysis, vmPFC GABA$_A$R BPs were used as regressors in the second level of analysis for the target contrasts, with the proportion of gray matter for each subject included as a control variable (Figure 3b). Thresholding for this regression map was $p < 0.005$ voxel-wise, $p < 0.05$ FWE cluster-wise corrected, $k \geqslant 334$. A conjunction analysis was performed to identify any overlapping activations between the whole-brain vmPFC GABA$_A$R-fMRI regression maps and the initial fMRI context interaction maps (Figure 3c). As areas throughout the bilateral sensorimotor cortex were identified, descriptive correlations were then performed intraregionally (Table 2) and interregionally with the vmPFC (Table 3); scatter plots of two selected regions are used to visually illustrate this relationship (Figure 3c).

Correlational analyses for PET-fMRI centered on the two functional conditions CerAv > SafeAv and CerNeu > SafeAv. The Cer > Safe contrast before the tone was used as a control period to further ensure any correlations noted arose from the context interaction period and not the anticipation of shock alone. Bonferroni corrections (alpha level of $p = 0.025$) were used for all *post-hoc* correlational analyses to reduce the risk of false-positive findings associated with multiple comparison testing. Furthermore, the Hotelling–Williams test for the equality of two dependent correlations was used to determine whether significant intra-regional correlations noted for one contrast was independent of the other (ie, CerAv > SafeAv and CerNeu > SafeNeu); hotelling T-squared testing for multivariate samples was used to determine whether significant correlations for one functional contrast was independent of signal changes in nearby clusters (Steiger, 1980; Williams, 1959). One-tailed tests were employed, given that the *a priori* hypothesis assumed a clear relationship between GABA$_A$Rs and BOLD signal changes. The results of these combined analyses are summarized in Figure 4.

RESULTS

Behavioral Results

Subjects rated the aversive tone (23.64 ± 17.58) as being more unpleasant after conditioning, on a 0–100 scale (where 0 is not unpleasant and 100 is the most unpleasant sound imaginable), compared with the neutral tone

Table 2 Intra-Regional GABA$_A$R BP and Aversion-Related fMRI Signal Changes (%)

Regions of interaction contrasts (MNI coordinates)	Contrasts		
	CerAv > SafeAv	**CerNeu > SafeNeu**	**PreCer > PreSafe**
Aversive interaction regions (Av(Cer > Safe))¬(Neu(Cer > Safe))	*r, p*	*r, p*	*r, p*
L sensory ctx (−13, −46, 63)	‡ **−0.530, 0.016**	−0.461, 0.041	−0.222, 0.348
L sensorimotor ctx (−18, −31, 69)	*‡ **−0556, 0.011**	−0.194, 0.412	−0.222, 0.349
R sensorimotor ctx (11, −28, 67)	*‡ **−0.630, 0.003**	−0.283, 0.227	0.014, 0.955
MCC (2, 2, 41)	−0.435, 0.055	0.012, 0.959	0.106, 0.656
L post insula (−38, −7, 0)	−0.336, 0.148	−0.376, 0.102	−0.117, 0.624
R post ins (37, −10, −7)	−0.208, 0.379	−0.311, 0.181	0.069, 0.773
R anterior/mid insula (36, 8, 7)	−0.350, 0.130	−0.202, 0.392	0.097, 0.684
L thal/midbrain (−9, −20, 3)	−0.493, 0.027	−0.241, 0.306	−0.198, 0.404
R thal (14, −14, 11)	−0.234, 0.322	0.375, 104	−0.174, 0.463
R midbrain (9, −19, −8)	−0.327, 0.159	0.084, 0.723	−0.107, 0.655
R sens assoc/par oper/SMG (56, −28, 27)	−0.100, 0.674	0.03, 0.901	0.072, 0.762
L sens assoc/par oper/SMG (−58, −25, 21)	0.083, 0.728	0.057, 0.811	−0.245, 0.289
L central oper (−55, 2, 3)	−0.117, 0.623	−0.083, 0.727	0.057, 0.810
L SMG/inferior parietal (−53, −34, 32)	0.351, 0.129	−0.050, 0.834	0.108, 0.651
Cerebellum (0, −49, −16)	−0.317, 0.174	−0.033, 0.889	0.009, 0.972
R mid insula (38, 11, −4)	−0.416, 0.068	−0.296, 0.205	0.143, 0.547
R parietal oper/post insula (34, −23, 18)	0.002, 0.994	0.124, 0.601	0.209, 0.375
L PCC (−14, −28, 39)	0.080, 0.737	0.413, 0.071	0.088, 0.714
Neutral interaction regions (Neu(Cer > Safe))¬(Av(Cer > Safe))			
L Sensorimotor cortex/L PCC (−10, −31, 63)	−0.498, 0.027	−0.471, 0.036	−0.243, 0.302
L Motor cortex (−17, −40, 69)	−0.290, 0.214	−0.072, 0.763	−0.199, 0.399
R Sensory cortex (16, −37, 76)	−0.387, 0.092	−0.401, 0.080	−0.163, 0.493
R Sensory cortex (18, −34, 67)	−0.470, 0.036	−0.397, 0.083	−0.196, 0.407
L posterior insula (−34, −23, 18)	−0.027, 0.909	−0.002, 0.994	0.102, 0.668
L posterior insula (−39, −22, −2)	−0.002, 0.993	−0.049, 0.836	−0.164, 0.488
R posterior insula (39, −17, 11)	−0.338, 0.145	−0.128, 0.590	−0.104, 0.663
R midbrain (9, −22, −12)	−0.102, 0.669	−0.063, 0.791	0.184, 0.483
L parietal operculum (−53, −30, 20)	−0.374, 104	−0.155, 0.515	−0.269, 0.251
R central operculum (59, −17, 19)	−0.184, 0.438	−0.040, 0.869	−0.362, 0.117
L cerebellum (−9, −42, −25)	0.072, 0.761	−0.035, 0.885	−0.231, 0.327
Overlapping regions (Av(Cer > Safe)) ∩ (Neu(Cer > Safe))			
L Sensory cortex (−17, −34, 70)	−0.414, 0.070	−0.104, 0.661	0.170, 0.473
R Sensorimotor cortex (9, −30, 66)	*‡ **−0.667, 0.001**	−0.284, 0.226	−0.187, 0.430
L posterior insula (−38, −18, −5)	−0.252, 0.283	−0.333, 0.151	0.016, 0.947
R posterior insula (35, −19, 15)	−0.439, 0.053	−0.224, 0.343	−0.199, 0.401
L parietal operculum (−49, −35, 25)	0.094, 0.695	0.109, 0.646	−0.027, 0.908
R parietal operculum (49, −25, 20)	−0.322, 0.166	−0.210, 0.375	−0.005, 0.983
Cerebellum (1, −46, −20)	−0.185, 0.434	−0.167, 0.482	−0.191, 421

Abbreviations: Av, aversive conditioned tone; BP, binding potential; Cer, certain shock; ctx, cortex; MCC, mid cingulate cortex; Neu, neutral conditioned tone; R/L, left/right; Safe, certain absence of shock.
Pearson correlations (r) between intra-regional GABAA receptor BP and % signal change differences for the two target contrasts (CerAv > SafeAv and CerNeu > SafeNeu), as well as for the pretone contrast (PreCer > Safe). Bolded numbers are significant following Bonferroni corrections; *significant (*p*; *p*-values) from CerNeu > SafeNeu contrast as determined by Hotelling–Williams test; †significant from CerAv > SafeAv contrast for nearest neutral interaction cluster. See Supplementary Table S3 for related information.

(10.01 ± 10.44), ($t = 4.9$; $p < 0.0001$). Shock ratings averaged 50.65 ± 13.26 across all subjects, which is consistent with moderate levels of experienced pain.

Parameter estimates (arbitrary units) for EDA (mean ± SE of the mean) for post-tone response in the four main target periods were: SafeAv (−0.16 ± 0.03), SafeNeu

(-0.17 ± 0.04), CerAv (0.16 ± 0.06) and CerNeu (0.17 ± 0.06). A 2×2 repeated measures ANOVA revealed a main effect of shock anticipation ($F(1,22) = 39.69$, $p < 0.0001$) but no main effect of tone ($F(1,22) = 0.005$, $p > 0.05$) or anticipation $\times$ tone interaction ($F(1,22) = 0.062$, $p > 0.05$). It is worth noting, however, that a main effect of shock anticipation ($F(1,22) = 5.10$, $p < 0.05$) and tone ($F(1,22) = 5.60$, $p < 0.05$), but no interaction ($F(1,22) = 0.16$, $p > 0.05$), were noted during the presentation of the tone. This is consistent with the subjective ratings above, associating both the certain shock anticipation and aversive tone with increased EDA responding:

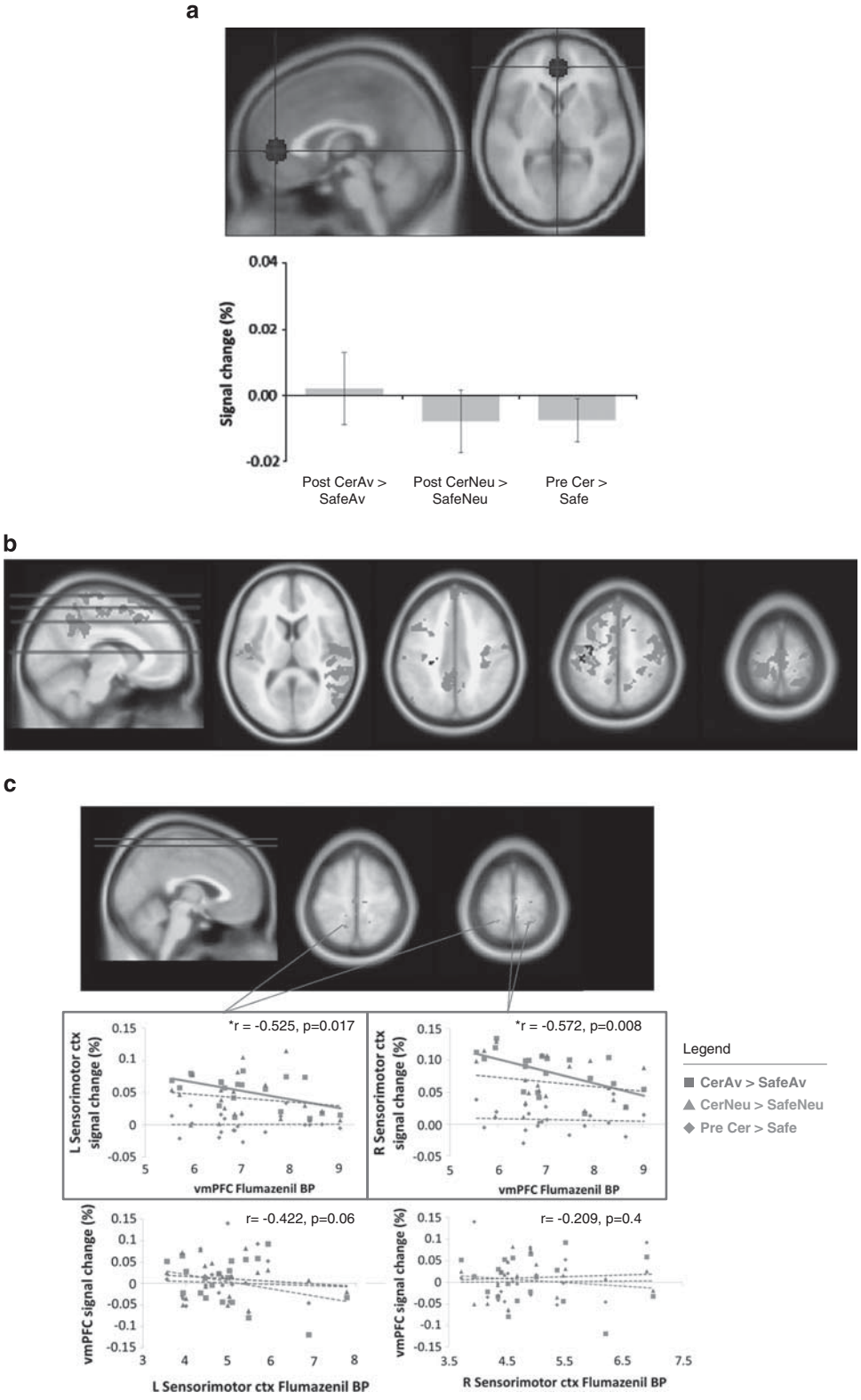

Figure 3 For caption please refer page 1445.

SafeAv (-0.27 ± 0.05), SafeNeu (-0.37 ± 0.06), CerAv (-0.20 ± 0.07), and CerNeu (-0.26 ± 0.05). Finally, a one-way repeated measures ANOVA of the period before the tone (ie, anticipation alone) also revealed an effect ($F(1,22) = 23.44$, $p < 0.0001$) of shock anticipation: certain (-0.28 ± 0.07) and safe (-0.61 ± 0.09).

Aversive Contex Interaction fMRI Results

As outlined in Figure 1b, analysis of the period of interest resulted in significant clusters ($p < 0.05$, FWE whole-brain corrected, $k > 10$) during shock anticipation following both aversive interaction and neutral interaction contrasts (ie, CerAv > SafeAv and CerNeu > SafeNeu) (Supplementary Table S1). There were no simple main effects at this threshold for conditioned tone valence (CerAv & SafeAv >< CerNeu & SafeNeu), though there were simple main effects for anticipation (CerAv & CerNeu >< SafeAv & SafeNeu); results not shown.

Interaction analyses using exclusive masking revealed significant clusters for both the aversive interaction ((CerAv > SafeAv)¬(CerNeu > SafeNeu)) and the neutral interaction ((CerNeu > SafeNeu)¬(CerAv > SafeAv)), as well as significant overlap using inclusive masking indicating signal changes unrelated to tone valence ((CerAv > SafeAv) ∩ (CerNeu > SafeNeu))—see Figure 2a, and corresponding Table 1 and Supplementary Table S1. Notably, sensorimotor cortex activation was stronger in the right hemisphere, consistent with left-ankle electrical stimulation. For completeness, the BOLD map for the pretone shock anticipation periods can be found in Supplementary Figure S1.

The extraction of mean percent signal changes from these context interaction-specific clusters (Figure 2b) suggested increased activations associated with each respective condition, although underscoring that these signal change differences do not appear related to activity occurring before the tone (ie, Pretone Cer > Safe; see Supplementary Table S2 for signal changes in all clusters). Although this

Table 3 Correlations Between GABA$_A$R BPs and BOLD Signal Changes Between vmPFC and Sensorimotor Cortices

Regions of interaction contrasts (MNI coordinates)	vmPFC GABA$_A$R BP × regional % signal change			Regional vmPFC GABA$_A$R BP × vmPFC % signal change		
	CerAv > SafeAv	**CerNeu > SafeNeu**	**Pre Cer > Safe**	**CerAv > SafeAv**	**CerNeu > SafeNeu**	**Pre Cer > Safe**
Aversive interaction regions (Av(Cer > Safe))¬(Neu(Cer > Safe))	*r, p*	*r, p*	*r, p*	*r, p*	*r, p*	*r, p*
L sensory ctx (−13, −46, 63)	* −**0.525, 0.017**	−0.177, 0.455	0.013, 0.956	−0.422, 0.064	−0.082, 0.732	−0.107, 0.654
L sensorimotor ctx (−18, −31, 69)	−**0.547, 0.013**	−0.281, 0.229	−0.137, 0.564	−0.121, 0.612	0.115, 0.630	−0.017, 0.994
R sensorimotor ctx (11, −28, 67)	* −**0.572, 0.008**	−0.196, 0.406	−0.065, 0.785	−0.209, 0.377	0.007, 0.976	−0.049, 0.838
Neutral interaction regions (Neu(Cer > Safe))¬(Av(Cer > Safe))						
L sensorimotor cortex/L PCC (−10, −31, 63)	−**0.514, 0.024**	−0.346, 0.147	−0.219, 0.367	−0.413, 0.079	0.086, 0.727	−0.013, 0.959
L motor cortex (−17, −40, 69)	* −**0.575, 0.008**	−0.242, 0.304	−0.039, 0.870	−0.028, 0.908	0.161, 0.497	−0.143, 0.547
R sensory cortex (16, −37, 76)	* −**0.538, 0.014**	−0.262, −0.265	−0.085, 0.722	−0.176, 0.457	−0.138, 0.561	−0.08, 0.736
R sensory cortex (18, −34, 67)	* −0.440, 0.052	−0.120, 0.613	−0.071, 0.765	−0.169, 0.476	0.166, 0.485	0.037, 0.877
Overlapping regions (Av(Cer > Safe)) ∩ (Neu(Cer > Safe))						
L sensory cortex (−17, −34, 70)	−0.473, 0.035	−0.208, 0.379	−0.046, 0.848	−0.070, 0.771	0.207, 0.381	0.085, 0.722
R sensorimotor cortex (9, −30, 66)	* −**0.566, 0.009**	−0.176, 0.458	−0.213, 0.367	−0.213, 0.367	0.083, 0.728	−0.086, 0.719

Pearson correlations (r) between vmPFC GABA$_A$ receptor BP and % signal change differences in the sensorimotor cortices, and vice versa, for the two target contrasts (CerAv > SafeAv and CerNeu > SafeNeu), as well as for the pretone contrast (PreCer > Safe). Bolded numbers are significant following Bonferroni corrections; *significant (*p*; *p*-values) from CerNeu > SafeNeu contrast as determined by Hotelling–Williams test. See Figure 4 for summary.

Figure 3 vmPFC ROI analysis. (a) signal change differences (%) in ventromedial prefrontal cortex (vmPFC): signal changes for an independent region of interest (ROI; MNI coordinates: x = 0, y = 46, z = 2) of the ventromedial prefrontal cortex for the two target contrasts (CerAv > SafeAv, CerNeu > SafeNeu) as well as for the pretone contrast (PreCer > Safe) were not significant. Error bars represent standard error of the mean. (b) whole-brain regression for vmPFC GABA$_A$R and context interaction fMRI BOLD maps: using the GABA$_A$R BPs in the vmPFC ROI as a regressor with whole-brain BOLD maps revealed correlations mainly in the aversive interaction period (CerAv > SafeAv, red). Only one cluster was noted for the neutral interaction contrast (blue) in the left motor cortex, though this overlapped largely with activity from both contrasts (green). Data are FWE whole-brain cluster corrected ($p < 0.005$), $k > 334$. See Supplementary Table S3 for supporting information. (c) overlap between whole-brain vmPFC GABA$_A$R regression and fMRI aversive interaction BOLD map: inclusive masking between the vmPFC GABA$_A$R BP regression map and the aversive interaction BOLD map revealed an overlap in bilateral sensorimotor cortices (top panel). For illustrative purposes, scatter plots showing signal changes correlating with vmPFC GABA$_A$R BPs for the CerAv > SafeAv contrast (red squares), but not for the CerNeu > SafeNeu (blue triangles) or Pre Cer > Safe (grey diamonds) contrasts, are shown (red outlined, middle panel) in two aversion interaction clusters. GABA$_A$R BPs within these same regions did not correlate with vmPFC signal changes (lower panel). Pearson correlations for the CerAv > SafeAv contrast are noted in the top right of each plot. See Table 3 for supporting information. Av, aversive conditioned tone; BP, binding potential; Cer, certain shock; ctx, cortex; dlPFC, dorsolateral prefrontal cortex; MCC, mid cingulate cortex; Neu, neutral conditioned tone; PCC, posterior cingulate cortex; R/L, left/right; Safe, certain absence of shock.

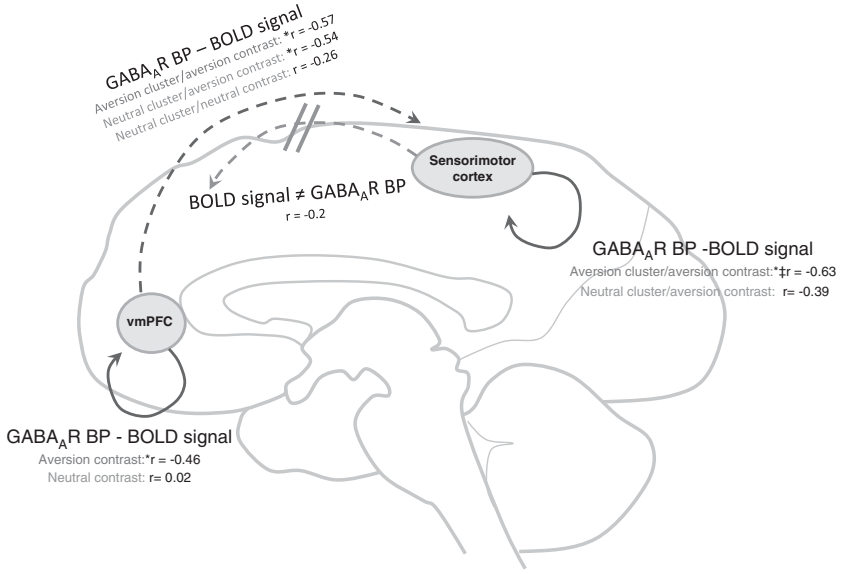

Figure 4 Illustration of multimodal findings for vmPFC-right sensorimotor cortex connection. Individual vmPFC GABA$_A$R BPs are negatively correlated (r = Pearson correlations) with aversion contrast BOLD signal changes, in both aversion and neutral interaction-selective clusters, in the right sensorimotor cortex. In addition, GABA$_A$R BPs within aversion-selective clusters of the sensorimotor cortex are correlated with signal changes from the same region. While these findings appear generalized across all sensorimotor clusters, the present Figure is an illustration of the right cluster only. Solid lines represent intra-regional, while dotted lines represent inter-regional,relationships. *Significant from CerNeu > SafeNeu contrast as determined by Hotelling–Williams paired correlation test; †Significant from CerAv > SafeAv contrast for nearest neutral interaction cluster as determined by Hotelling's T-squared test for two multivariate dependent samples. See Table 3 for related information. BP, binding potential; GABA, gamma-aminobutyric acid; GABA$_A$R, GABA A receptors; PET, positron emission tomography.

pattern (eg, greater differences in activation from CerAv > SafeAv compared with CerNeu > SafeNeu) was consistent with all aversive interaction clusters, some neutral interaction clusters (eg, right sensory cortex) showed an opposite pattern, suggesting relative signal change decreases within these regions from the aversive to neutral contrasts.

fMRI-PET Results

Intra-regional GABA$_A$R BPs were parametrically correlated with mean percent signal change differences (CerAv > SafeAv and CerNeu > SafeNeu) within three sensorimotor cortex regions selective for the aversive interaction ((Av(-Cer > Safe))¬(Neu(Cer > Safe)). These included the right sensorimotor (Table 2; x, y, and z in MNI space: 11, −28, 67; $r = -0.630$, $p = 0.003$), left sensorimotor (−18, −31, 69; $r = -0.556$, $p = 0.011$), and left sensory (−13, −46, 63; −0.530, $p = 0.016$) cortical clusters. However, the signal change difference in the left sensory cluster (−13, −46, and 63) did not reach significance between the aversive and neutral interaction contrasts, as determined by the Hotelling–Williams test. In addition, one cluster within the right sensorimotor cortex identified as non-specific for tone value from the (Av(Cer > Safe)) ∩ (Neu(Cer > Safe)) expression also showed a significant negative correlation ($r = -0.667$, $p = 0.001$) for GABA$_A$R BPs and signal change differences in the CerAv > SafeAv condition. Importantly, these clusters also showed correlations of BPs and signal changes that were independent of nearby sensorimotor clusters from the neutral interaction (Neu(Cer > Safe))¬(Av(Cer > Safe))—except for one right sensorimotor cortex cluster from the aversive interaction and a small (k = 21) neighbor from the neutral interaction.

vmPFC ROI Analyses: fMRI-PET Results

As shown in Figure 3a, mean percent signal changes extracted from the independently selected vmPFC ROI (see Materials and methods for details) were not significant for the contrasts of interest following paired sample *t*-tests ($p > 0.05$). This result is consistent with other studies noting little BOLD activity in the vmPFC during the perception of aversive stimuli (Hayes and Northoff, 2011, Hayes and Huxtable, 2012).

Inputting individual vmPFC GABA$_A$R BPs as regressors in the interaction contrasts revealed significant correlations at the whole-brain level ($p < 0.005$, FWE whole-brain cluster corrected, k > 334) between vmPFC GABA$_A$R BP and aversive interaction signal change differences (Figure 3b). Only one cluster was noted for the neutral interaction contrast in the left motor cortex, though this overlapped largely with activity from both contrasts (see Supplementary Table S3 for all cluster-related details).

Inclusive masking between the aversive interaction BOLD and vmPFC GABA$_A$R BP regression maps revealed significant overlap only in bilateral sensorimotor cortices (Figure 3c; no results were found for the neutral interaction). Sample scatter plots further illustrate the Pearson's correlations (Table 3). Interestingly, this same relationship was noted also for sensorimotor regions selectively identified by the neutral context interaction (Neu(Cer > Safe))¬(Av(Cer > Safe))—showing that vmPFC GABA$_A$R BPs correlated with the aversion-related signal changes across

all sensorimotor cortex clusters. The reverse relationship was not seen, as $GABA_AR$ BPs from the bilateral sensorimotor clusters did not correlate with any signal changes from the vmPFC (Figure 3c and Table 3).

Although the signal change differences in the vmPFC were not significant, the correlation of vmPFC $GABA_AR$ BPs to vmPFC signal change differences was significant for the aversive ($r = -0.462$, $p = 0.040$; but not neutral, $r = 0.02$, $p = 0.9$) interaction contrast. Although this correlation must be considered at the trend level, given that it was above the Bonferroni correction level, it was nonetheless significantly different from the correlation noted for the CerNeu > SafeNeu contrast as determined by the Hotelling–Williams test ($p = 0.03$).

DISCUSSION

Neuroimaging studies on aversion show consistent activity in the midcingulate cortex (MCC), motor cortex, insula, thalamus, supramarginal gyrus, and midbrain (Grupe *et al*, 2012; Hayes and Northoff 2012; Hayes and Northoff 2011; Nitschke *et al*, 2006; Onoda *et al*, 2008). Our results are consistent with this activity, as seen especially during the anticipation period before the presentation of the tones (Pre Cer > Safe; see Figure 1b for design and Supplementary Figure S1 for the pretone contrast). Importantly, our multimodal design extended these findings by using passive, unpredictable, pre-conditioned tones as cues (adapted from Dunsmoor *et al*, 2008 and Knight *et al*, 2009, and supported behaviorally, physiologically, and through differential BOLD results) to reveal unique brain-related modulations of the shock anticipation (Figure 2a and Table 1)—ie, differential activations between the aversive Av(Cer > Safe) and neutral Neu(Cer > Safe) interaction contrasts. These results suggest that information related to aversive context, which is not necessarily tied to probabilistic outcomes (ie, the tones did not reflect the probability of shock), is reflected in subtle changes throughout this aversion-related network. Moreover, these context-dependent differences in aversive processing appear to be partly controlled by a GABAergic mechanism both locally (ie, within sensorimotor cortex) and distally (ie, from the vmPFC) as is discussed further below.

Aversive Context Interaction BOLD Activity

These BOLD responses are consistent with typical aversion-related activity (as noted above, see Grupe *et al*, 2012). Additional activity within sensorimotor cortices and posterior insula/parietal operculum were noted, which are known to be involved in aversive and non-aversive somatosensory (Bingel *et al*, 2003; Mouraux *et al*, 2011) processing. These regions have been shown to display potentiated responding to non-painful, aversive, somatosensory stimuli during the anticipation of thermal pain (Sawamoto *et al*, 2000), supporting their involvement in the modulation of aversive sensory information. Alternately, absent/decreased activity in some regions, such as in mid/anterior insula and MCC, in the neutral interaction could reflect relative decreases in signal change in these regions. In support of this interpretation, sensorimotor and posterior insula clusters identified specifically in the neutral contrast showed lower signal change differences when compared with the aversive interaction (see Figure 2b; Supplementary Table S2). These are consistent with relative deactivations (eg, see Hayes and Huxtable, 2012) previously noted in the somatosensory cortex surrounding the primary site of activation (related to the threat of shock on the left ankle in this case) as well as ipsilateral to it (Drevets *et al*, 1995; Klingner *et al*, 2011).

Modulation of Shock Anticipation Activity by Sensorimotor $GABA_ARs$

It was found that intra-regional $GABA_AR$ BPs in the sensorimotor cortex were predictive of aversive interaction BOLD signal changes (Table 2), suggesting that GABA is partly involved in mediating the aversive context interaction within these regions. This is contrary to our initial hypothesis that $GABA_AR$ BPs throughout the network would correlate with signal changes, but supports a role for selected regions of sensorimotor cortex in mediating modality-specific responses to emotional stimuli (Mouraux *et al*, 2011). These results show that $GABA_AR$ availability/function in the sensory cortex is predictive of brain reactivity for the aversive anticipation–aversive cue context interaction (Table 2)—ie, as $GABA_AR$ availability/function increases, signal change differences decrease. Moreover, this relationship is noted only in regions that were selectively identified from the aversive (and not neutral) interaction, suggesting that $GABA_ARs$ have differential roles in the processing of aversive context-related information throughout subregions of the sensorimotor cortex.

Specifically, we found negative correlations throughout bilateral sensorimotor cortex for regions related only to the aversive interaction, as well as in one cluster whose activity was unrelated to tone type (an overlapping region noted in green in Figure 2a). Interestingly, although there is some evidence that emotional cues can differentially modulate responses in primary and secondary sensorimotor cortices (Montoya and Sitges, 2006; Van den Stock *et al*, 2011), this is the first indication that $GABA_ARs$ might be involved in mediating this difference. This suggests that increased $GABA_AR$ availability/function within the bilateral sensorimotor cortex results in less responsivity (and/or greater inhibition), specifically, within the subregions identified in the present study.

GABA is the main inhibitory neurotransmitter in the nervous system and has been associated with decreases in BOLD responses in both animal (Chen *et al*, 2005) and human (Muthukumaraswamy *et al*, 2011; Northoff *et al*, 2007) studies. The primary fast-acting target of GABA is the ionotropic $GABA_AR$, and it is well-known to be involved in the inhibition of cellular activity, particularly through its increasing of inhibitory postsynaptic potentials (Petrini *et al*, 2011). This is in line with the notion that $GABA_ARs$ within aversion interaction sensorimotor subregions may predict enhanced inhibition, as reflected by lower signal change differences from the interaction contrasts in individuals with higher $GABA_AR$ BPs. This interpretation is also consistent with a study showing that FMZ binding in human sensorimotor cortex is related to intra-cortical inhibition (Capaday *et al*, 2000).

Modulation of Context-Related Aversive Activity by vmPFC GABA

The vmPFC (Figure 3a) was recently hypothesized as being essential in the integration of emotion-related contextual information (Roy *et al*, 2012). The authors described this process in terms of 'the generation of affective meaning' to explain apparently different functions across a wide range of studies. This interpretation is consistent with our study identifying vmPFC GABA$_A$Rs as being involved in context-dependent aversion-related processing. The availability/function of vmPFC GABA$_A$Rs appears to predict the responsivity to contextual aversive stimuli regardless of which sensorimotor cortex regions they came from (Figure 3c, Table 3; ie, regions from both the aversive or neutral interaction contrasts). Importantly, the relationship between vmPFC/intra-regional GABA$_A$R BPs and sensorimotor signal changes appears to be unidirectional, as sensorimotor BPs do not predict signal changes in the vmPFC (Figure 3c, Table 3). We suggest that these results are best understood by taking GABA$_A$R BP as a measure of inhibitory capacity (ie, the intra-regional ability to be inhibited). All correlations were negative, implying that individual increases in GABA$_A$R availability/function are related to an increased capacity to inhibit brain function, as reflected in lower degrees of responsive signal changes in the aversive context interaction.

The notion of the vmPFC as an integrator of emotional and contextual information is consistent with what is known about mPFC GABA in rats, as inactivation, through the microinjection of GABA mimetic drugs, is associated with increased anxiety, disrupted decision making abilities (de Visser *et al*, 2011), and reduced processing speed and cognitive flexibility (Enomoto *et al*, 2011). Evidence also suggests that the mPFC inhibits aversion-related activity through direct inhibition of limbic regions (Quirk *et al*, 2003). Furthermore, it has been suggested that mPFC pain-related deactivations depend on the stimulation of both glutamatergic mGluR1/5 and GABA$_A$Rs (Ji and Neugebauer, 2011), ultimately, resulting in GABAergic inhibition of mPFC cells. Finally, a functional MRS study showed increases in vmPFC GABA following exposure to painful stimuli in healthy humans (Kupers *et al*, 2009), consistent with numerous early animal studies (Miyauchi *et al*, 1988). These studies support our findings that the vmPFC GABA$_A$R BPs in humans are correlated to aversive processing, but, in addition, show that the contextual information must also be considered. In particular, our study demonstrated that brain responses related to shock anticipation, though highly aversive, did not correlate with GABA$_A$R measures following the presentation of the neutral tone (in contrast to the aversive tone).

Limitations and Future Directions

Methodologically, the presentation of passive stimuli (in the absence of any task) was used to target basic aversive processing, however, we must acknowledge that any study using aversive stimuli may result in the use of cognitive-based coping strategies. Nonetheless, activations associated with the emotional regulation of unpleasant stimuli, such as in the dorsolateral prefrontal and orbitofrontal cortices, were not noted in the present study (Eippert *et al*, 2007). Also, given the correlational analyses used, we aimed to reduce the risk of false-positive findings through supporting approaches (eg, fMRI-PET at the whole-brain and ROI level), through consideration of the animal literature, and by using appropriate tests to determine the equality between two dependent correlations (see Materials and methods for additional information). Despite these caveats, we showed significant and selective differences between the conditions, which helped to specify the interactions both regionally and neurochemically.

Interpretations of the present data are aversion-related, but should not be considered aversion-specific. For instance, because highly rewarding stimuli were not used in the present study, these results could be explained in terms of salience-related processing. Indeed, the MCC and insula are considered key regions of a salience network (Seeley *et al*, 2007), and some of the present activations (eg, anterior cingulate and temporoparietal cortex) seem to overlap with those identified in other studies on salience-related processing (Downar *et al*, 2003). Although the issue of salience is often raised (and was not directly addressed in the present study), there is much evidence in animals (though relatively little in humans) to identify reward- and aversion-related processing as involving distinct, parallel, and sometimes overlapping, circuitry (Amemori and Graybiel, 2012; Carlezon and Thomas, 2009; Hayes *et al*, 2011); future studies should aim to disentangle these processes in humans.

Some areas involved in reward-related processing (eg, vmPFC) are also key in so-called task-negative and/or self-related networks (Kringelbach and Berridge, 2009; Northoff and Hayes, 2011). As mind wandering and self-reflections may be associated with negative emotional states (Smallwood *et al*, 2009), aversion-related processing may also interact with task-negative activity. The present data are in line with this notion, though not tested directly, as the vmPFC (a typical task-negative region) was involved in processing the differentiation of the aversive context interactions. A better understanding of interactions between putative task-negative and -positive regions may lead to novel insights regarding emotional processing in relation to healthy and abnormal brain functioning (Northoff *et al*, 2010). For example, functional connectivity between the mPFC and nucleus accumbens may predict the transition from acute to chronic pain (Baliki *et al*, 2012). Also, altered mPFC deactivations are linked to the severity of negative emotionality in major depressive disorder (Grimm *et al*, 2009), and patients with generalized social phobia show increased mPFC activity to negative, self-related, comments (Blair *et al*, 2008). Although the vmPFC is considered a task-negative region, this study and others (Duncan *et al*, 2011; Quirk *et al*, 2003) show a relationship to task-positive regions that question the current nomenclature (Northoff *et al*, 2010; Spreng, 2012).

CONCLUSION

In summary, the present study revealed an aversive context interaction across many brain regions associated with aversion-related processing. The modulation noted in some

sensorimotor cortex subregions, in particular, appears to be mediated by a GABAergic mechanism. Furthermore, vmPFC $GABA_A$Rs also predict sensorimotor responsivity to aversive stimuli, though the results under the current experimental conditions suggest the vmPFC has a more general context-related role. Beyond basic principles of aversive brain function, future investigations could use the present findings for neuropsychiatric populations. For instance, though much research has emphasized the impact of cognitive processing abnormalities, there is growing support for focusing more on understanding the interplay between sensorimotor activity and basic emotion circuitry in disorders as apparently disparate as depression or fibromyalgia (Canbeyli, 2010; Montoya *et al*, 2005). Robustly activating the aversion-related system before using aversive cues as probes may help to identify subtle network differences across individuals, particularly patients showing altered aversion-related processing.

ACKNOWLEDGEMENTS

We thank Andrea Perna and Katarina Dedovic for their help with subject recruitment, and the staff at the UNF and MNI for their skillful assistance. Also, we would like to thank Étienne Vachon-Presseau for his technical expertise regarding electrical stimulation and Oliver Lyttelton for his assistance with anatomical image acquisition. The work was supported by grants to GN from the Canadian Institutes of Health Research (CIHR), the Michael Smith Foundation, and Hope for Depression research foundation (HDRF/ISAN). DJH was funded through a CIHR Postdoctoral Fellowship.

DISCLOSURE

The authors declare no conflict of interest.

REFERENCES

Amemori K, Graybiel AM (2012). Localized microstimulation of primate pregenual cingulate cortex induces negative decision-making. *Nat Neurosci* **15**: 776–785.

Bach DR, Flandin G, Friston KJ, Dolan RJ (2010). Modelling event-related skin conductance responses. *Int J Psychophysiol* **75**: 349–356.

Bach DR, Flandin G, Friston KJ, Dolan RJ (2009). Time-series analysis for rapid event-related skin conductance responses. *J Neurosci Methods* **184**: 224–234.

Baliki MN, Petre B, Torbey S, Herrmann KM, Huang L, Schnitzer TJ *et al* (2012). Corticostriatal functional connectivity predicts transition to chronic back pain. *Nat Neurosci* **15**: 1117–1119.

Bingel U, Quante M, Knab R, Bromm B, Weiller C, Buchel C (2003). Single trial fMRI reveals significant contralateral bias in responses to laser pain within thalamus and somatosensory cortices. *Neuroimage* **18**: 740–748.

Blair K, Geraci M, Devido J, McCaffrey D, Chen G, Vythilingam M *et al* (2008). Neural response to self- and other referential praise and criticism in generalized social phobia. *Arch Gen Psychiatry* **65**: 1176–1184.

Canbeyli R (2010). Sensorimotor modulation of mood and depression: an integrative review. *Behav Brain Res* **207**: 249–264.

Capaday C, Richardson MP, Rothwell JC, Brooks DJ (2000). Long-term changes of GABAergic function in the sensorimotor cortex of amputees. A combined magnetic stimulation and 11C-flumazenil PET study. *Exp Brain Res* **133**: 552–556.

Carlezon WA Jr., Thomas MJ (2009). Biological substrates of reward and aversion: a nucleus accumbens activity hypothesis. *Neuropharmacology* **56**(Suppl 1): 122–132.

Chan T, Kyere K, Davis BR, Shemyakin A, Kabitzke PA, Shair HN *et al* (2011). The role of the medial prefrontal cortex in innate fear regulation in infants, juveniles, and adolescents. *J Neurosci* **31**: 4991–4999.

Chen Z, Silva AC, Yang J, Shen J (2005). Elevated endogenous GABA level correlates with decreased fMRI signals in the rat brain during acute inhibition of GABA transaminase. *J Neurosci Res* **79**: 383–391.

Ciocchi S, Herry C, Grenier F, Wolff SB, Letzkus JJ, Vlachos I *et al* (2010). Encoding of conditioned fear in central amygdala inhibitory circuits. *Nature* **468**: 277–282.

de Visser L, Baars AM, van 't Klooster J, van den Bos R (2011). Transient inactivation of the medial prefrontal cortex affects both anxiety and decision-making in male wistar rats. *Front Neurosci* **5**: 102.

Delgado MR, Jou RL, Phelps EA (2011). Neural systems underlying aversive conditioning in humans with primary and secondary reinforcers. *Front Neurosci* **5**: 71.

Downar J, Mikulis DJ, Davis KD (2003). Neural correlates of the prolonged salience of painful stimulation. *Neuroimage* **20**: 1540–1551.

Drevets WC, Burton H, Videen TO, Snyder AZ, Simpson JR Jr., Raichle ME (1995). Blood flow changes in human somatosensory cortex during anticipated stimulation. *Nature* **373**: 249–252.

Duncan NW, Enzi B, Wiebking C, Northoff G (2011). Involvement of glutamate in rest-stimulus interaction between perigenual and supragenual anterior cingulate cortex: a combined fMRI-MRS study. *Hum Brain Mapp* **32**: 2172–2182.

Dunsmoor JE, Bandettini PA, Knight DC (2008). Neural correlates of unconditioned response diminution during Pavlovian conditioning. *Neuroimage* **40**: 811–817.

Eippert F, Veit R, Weiskopf N, Erb M, Birbaumer N, Anders S (2007). Regulation of emotional responses elicited by threat-related stimuli. *Hum Brain Mapp* **28**: 409–423.

Enomoto T, Tse MT, Floresco SB (2011). Reducing prefrontal gamma-aminobutyric acid activity induces cognitive, behavioral, and dopaminergic abnormalities that resemble schizophrenia. *Biol Psychiatry* **69**: 432–441.

Fiorelli R, Rudolph U, Straub CJ, Feldon J, Yee BK (2008). Affective and cognitive effects of global deletion of alpha3-containing gamma-aminobutyric acid-A receptors. *Behav Pharmacol* **19**: 582–596.

Frey KA, Holthoff VA, Koeppe RA, Jewett DM, Kilbourn MR, Kuhl DE (1991). Parametric in vivo imaging of benzodiazepine receptor distribution in human brain. *Ann Neurol* **30**: 663–672.

Grimm S, Boesiger P, Beck J, Schuepbach D, Bermpohl F, Walter M *et al* (2009). Altered negative BOLD responses in the default-mode network during emotion processing in depressed subjects. *Neuropsychopharmacology* **34**: 932–843.

Grupe DW, Oathes DJ, Nitschke JB (2012). Dissecting the anticipation of aversion reveals dissociable neural networks. *Cereb Cortex* (e-pub ahead of print) doi:10.1093/cercor/bhs175.

Hayes DJ, Hoang J, Greenshaw AJ (2011). The role of nucleus accumbens shell GABA receptors on ventral tegmental area intracranial self-stimulation and a potential role for the 5-HT2C receptor. *J Psychopharmacol* **25**: 1661–1675.

Hayes DJ, Huxtable AG (2012). Interpreting deactivations in neuroimaging. *Front Psychol* **3**: 27.

Hayes DJ, Northoff G (2012). Common brain activations for painful and nonpainful aversive stimuli. *BMC Neurosci* **13**: 60.

Hayes DJ, Northoff G (2011). Identifying a network of brain regions involved in aversion-related processing: a cross-species translational investigation. *Front Integr Neurosci* **5**: 49.

Ji G, Neugebauer V (2011). Pain-related deactivation of medial prefrontal cortical neurons involves mGluR1 and GABA(A) receptors. *J Neurophysiol* **106**: 2642–2652.

Johnson LR, Hou M, Prager EM, Ledoux JE (2011). Regulation of the Fear Network by Mediators of Stress: Norepinephrine Alters the Balance between Cortical and Subcortical Afferent Excitation of the Lateral Amygdala. *Front Behav Neurosci* **5**: 23.

Klingner CM, Huonker R, Flemming S, Hasler C, Brodoehl S, Preul C *et al* (2011). Functional deactivations: multiple ipsilateral brain areas engaged in the processing of somatosensory information. *Hum Brain Mapp* **32**: 127–140.

Knight DC, Waters NS, King MK, Bandettini PA (2009). Learning-related diminution of unconditioned SCR and fMRI signal responses. *Neuroimage* **49**: 843–848.

Kringelbach ML, Berridge KC (2009). Towards a functional neuroanatomy of pleasure and happiness. *Trends Cogn Sci* **13**: 479–487.

Kupers R, Danielsen ER, Kehlet H, Christensen R, Thomsen C (2009). Painful tonic heat stimulation induces GABA accumulation in the prefrontal cortex in man. *Pain* **142**: 89–93.

Lehner M, Taracha E, Skorzewska A, Turzynska D, Sobolewska A, Maciejak P *et al* (2008). Expression of c-Fos and CRF in the brains of rats differing in the strength of a fear response. *Behav Brain Res* **188**: 154–167.

Lehner M, Wislowska-Stanek A, Skorzewska A, Maciejak P, Szyndler J, Turzynska D *et al* (2010). Differences in the density of GABA-A receptor alpha-2 subunits and gephyrin in brain structures of rats selected for low and high anxiety in basal and fear-stimulated conditions, in a model of contextual fear conditioning. *Neurobiol Learn Mem* **94**: 499–508.

Miyauchi T, Dworkin SI, Co C, Smith JE (1988). Specific effects of punishment on amino acids turnover in discrete rat brain regions. *Pharmacol Biochem Behav* **31**: 523–531.

Montoya P, Sitges C (2006). Affective modulation of somatosensory-evoked potentials elicited by tactile stimulation. *Brain Res* **1068**: 205–212.

Montoya P, Sitges C, Garcia-Herrera M, Izquierdo R, Truyols M, Blay N *et al* (2005). Abnormal affective modulation of somatosensory brain processing among patients with fibromyalgia. *Psychosom Med* **67**: 957–963.

Mouraux A, Diukova A, Lee MC, Wise RG, Iannetti GD (2011). A multisensory investigation of the functional significance of the 'pain matrix'. *Neuroimage* **54**: 2237–2249.

Muthukumaraswamy SD, Evans CJ, Edden RA, Wise RG, Singh KD (2011). Individual variability in the shape and amplitude of the BOLD-HRF correlates with endogenous GABAergic inhibition. *Hum Brain Mapp* **33**: 455–465.

Nitschke JB, Sarinopoulos I, Mackiewicz KL, Schaefer HS, Davidson RJ (2006). Functional neuroanatomy of aversion and its anticipation. *Neuroimage* **29**: 106–116.

Northoff G, Hayes DJ (2011). Is our self nothing but reward? *Biol Psychiatry* **69**: 1019–1025.

Northoff G, Qin P, Nakao T (2010). Rest-stimulus interaction in the brain: a review. *Trends Neurosci* **33**: 277–284.

Northoff G, Walter M, Schulte RF, Beck J, Dydak U, Henning A *et al* (2007). GABA concentrations in the human anterior cingulate cortex predict negative BOLD responses in fMRI. *Nat Neurosci* **10**: 1515–1517.

Onoda K, Okamoto Y, Toki S, Ueda K, Shishida K, Kinoshita A *et al* (2008). Anterior cingulate cortex modulates preparatory activation during certain anticipation of negative picture. *Neuropsychologia* **46**: 102–110.

Petrini EM, Nieus T, Ravasenga T, Succol F, Guazzi S, Benfenati F *et al* (2011). Influence of GABAAR monoliganded states on GABAergic responses. *J Neurosci* **31**: 1752–1761.

Piche M, Arsenault M, Rainville P (2010). Dissection of perceptual, motor and autonomic components of brain activity evoked by noxious stimulation. *Pain* **149**: 453–462.

Qin P, Northoff G (2011). How is our self related to midline regions and the default-mode network? *Neuroimage* **57**: 1221–1233.

Quirk GJ, Likhtik E, Pelletier JG, Pare D (2003). Stimulation of medial prefrontal cortex decreases the responsiveness of central amygdala output neurons. *J Neurosci* **23**: 8800–8807.

Roy M, Shohamy D, Wager TD (2012). Ventromedial prefrontal-subcortical systems and the generation of affective meaning. *Trends Cogn Sci* **16**: 147–156.

Rudolph U, Knoflach F (2011). Beyond classical benzodiazepines: novel therapeutic potential of GABAA receptor subtypes. *Nat Rev Drug Discov* **10**: 685–697.

Salmi E, Aalto S, Hirvonen J, Langsjo JW, Maksimow AT, Oikonen V *et al* (2008). Measurement of GABAA receptor binding in vivo with [11C]flumazenil: a test-retest study in healthy subjects. *NeuroImage* **41**: 260–269.

Sawamoto N, Honda M, Okada T, Hanakawa T, Kanda M, Fukuyama H *et al* (2000). Expectation of pain enhances responses to nonpainful somatosensory stimulation in the anterior cingulate cortex and parietal operculum/posterior insula: an event-related functional magnetic resonance imaging study. *J Neurosci* **20**: 7438–7445.

Seeley WW, Menon V, Schatzberg AF, Keller J, Glover GH, Kenna H *et al* (2007). Dissociable intrinsic connectivity networks for salience processing and executive control. *J Neurosci* **27**: 2349–2356.

Smallwood J, Fitzgerald A, Miles LK, Phillips LH (2009). Shifting moods, wandering minds: negative moods lead the mind to wander. *Emotion* **9**: 271–276.

Smith SM, Jenkinson M, Woolrich MW, Beckmann CF, Behrens TE, Johansen-Berg H *et al* (2004). Advances in functional and structural MR image analysis and implementation as FSL. *Neuroimage* **23**(Suppl 1): S208–S219.

Spreng RN (2012). The fallacy of a 'task-negative' network. *Front Psychol* **3**: 145.

Steiger JH (1980). Tests for comparing elements of a correlation matrix. *Psychological Bulletin* **87**: 245–251.

Thompson BM, Baratta MV, Biedenkapp JC, Rudy JW, Watkins LR, Maier SF (2010). Activation of the infralimbic cortex in a fear context enhances extinction learning. *Learn Mem* **17**: 591–599.

Van den Stock J, Tamietto M, Sorger B, Pichon S, Grezes J, de Gelder B (2011). Cortico-subcortical visual, somatosensory, and motor activations for perceiving dynamic whole-body emotional expressions with and without striate cortex (V1). *Proc Natl Acad Sci USA* **108**: 16188–16193.

Wiebking C, Duncan NW, Qin P, Hayes DJ, Lyttelton O, Gravel P *et al* (2012). External awareness and GABA-A multimodal imaging study combining fMRI and [(18) F]flumazenil-PET. *Hum Brain Mapp* (e-pub ahead of print) doi:10.1002/hbm.22166.

Williams EJ (1959). The comparison of regression variables. *J R Stat Soc B* **21**: 396–399.

Supplementary Information accompanies the paper on the Neuropsychopharmacology website (http://www.nature.com/npp)